processes

MDPI

Article

Experimental Investigation of the Effect of Evaporator and Heat Exchanger Types on Heat Pump Performance Using the Taguchi Method

Fadime Şimşek * and Mehmet Akkoca

Department of Mechanical Engineering, Ataturk University, Erzurum 25240, Turkey
* Correspondence: fadimesimsek@atauni.edu.tr

Abstract

In this study, a modified heat pump system has been designed for heating applications in cold climate regions, enabling the replacement of system components such as the evaporator and heat exchanger within the same system. In this modified heat pump system, which uses R407C and R417A refrigerants instead of the restricted R22 refrigerant, the optimal system conditions that provide the best performance were determined using the Taguchi experimental method, prepared using five different parameters. As a result of the experiments, the optimum operating conditions of the system were determined from the analysis of variance table obtained by considering the COP and exergetic efficiency values. As a result, it was determined that the COP and exergetic efficiency values were higher in the case of using the 8 mm lamella spacing evaporator type and horizontal heat exchanger type.

Keywords: heat pump; COP; exergetic efficiency; Taguchi method

1. Introduction

Due to the world's increasing population and urbanization rate, the need for energy is increasing day by day in the utilization of a large part of plant and animal resources. For this reason, many studies are being carried out in the field of technology in order to find new energy sources, transform energy into efficient energy, and transfer it.

Global warming, as a result of excessive fossil fuel consumption, causes environmental problems such as melting glaciers, rising sea levels, acid precipitation, stratospheric ozone depletion, and the greenhouse effect. It is seen that potential solutions to these problems will be possible with renewable energy technologies [1]. For this purpose, effective methods have been introduced to combat global warming and reduce greenhouse gas emissions and fossil fuel consumption. Among these, heat pumps using vapor compression provide a practical way to lower primary energy use and recover energy from waste heat sources [2]. Heat pumps are preferred for many reasons, such as their high efficiency, their ability to be used for both heating and cooling purposes, their ability to utilize different heat sources, their environmental friendliness, and their ability to be designed and manufactured according to different heat needs and operating conditions. However, in order to increase the use and development of vapor compression heat pumps, studies to reduce the negative effects of global warming caused by refrigerants that act as heat transfer have recently been a common research topic.

All HCFCs containing the ozone-depleting substance chlorine, including R22, which is extensively used in the heat pump industry, are banned by the Montreal Protocol [3,4]. The

Check for updates

Academic Editor: Blaž Likozar

Received: 3 March 2026
Revised: 18 March 2026
Accepted: 20 March 2026
Published: 27 March 2026

Copyright: © 2026 by the authors. Licensee MDPI, Basel, Switzerland. This article is an open access article distributed under the terms and conditions of the Creative Commons Attribution (CC BY) license.

Kyoto Protocol has been proposed to solve this problem arising from hydrofluorocarbon refrigerants, which cause global warming and are preferred due to their thermodynamic and transportation properties [5]. In short, following the Montreal Protocol and the Kyoto Protocol, these gases are scheduled to be completely phased out by 2040 in 147 countries in order to mitigate the environmental damage they cause to the ozone layer or through the greenhouse effect [6].

HFC (hydrofluorocarbon) refrigerants, proposed as an alternative to the gradually banned R22 refrigerant, have significant advantages over CFC (chlorofluorocarbon) and HCFC (hydrochlorofluorocarbon) refrigerants in most applications.

However, hydrofluorocarbon-based refrigerants, which are already widely used in the market as alternatives to R22, also have characteristics such as a high global warming potential (GWP) and the need for higher operating pressure levels compared to other refrigerants. However, since they do not deplete the ozone layer, their use in heat pumps is of great importance in preventing future climate issues.

As an alternative to R22, R417A refrigerant, trade name Isceon 59, which belongs to the HFC group, was used because it does not damage the ozone layer, does not require changing the type of lubricant, and does not require significant changes in the system [7]. In addition, this refrigerant is preferred because the high energy efficiency of HFCs largely offsets the global warming potential. In addition, in Sarbu's study, according to TEWI (total equivalent warming effect) data, the literature study on R417A and R407C refrigerants, which are preferred because they show a deviation of approximately 2% compared to R22, is given in Table 1 [8].

Table 1. Literature studies conducted on alternative refrigerants used in heat pumps.

Reference	Refrigerant	Approach/System	Conclusions
Aprea et al. [7]	R22, R417A	Experimental/ Both cooling and heat pump	The COP and exergetic efficiency of the system were found to be higher than R417A when R22 was used. The COP of R22 is about 18% higher than that of R417A on the water cooling system side and 15% higher on the heat pump side.
Fannou et al. [9]	R22, R410A, R407C	Experimental/ Direct expansion geothermal evaporator	It is stated that the evaporator pressure drop of R407C is greater than R410A, and the pressure drop of R22 is greater than R407C and R410A. It is concluded that R407C is the best refrigerant to replace R22.
Messineo et al. [10]	R22,R417A, R404A, R407C	Experimental/ Heat pump	R407C and R417A zeotropic blends performed no better than R22.
Joudi and Al-amir [11]	R22,R290, R407C, R410A	Experimental/ klima sistemi	It is stated that the refrigerant with the highest compression ratio is R407C and R407C has the closest performance to R22, followed by R410A
Ergün et al. [12]	R22, R-417A, R-438A	Analytical/ Heat pump	R-438A, which was found to be the best alternative refrigerant, was found to have the highest COP value. It was also found that R-438A is more efficient than R-417A according to condenser and compressor loads.
Cingiz et al. [13]	R22,R417A, R422A, R422D, R438A	Experimental/ Heat pump	It was determined that the best performance in a heat pump system operating with R22 refrigerant was obtained from R438A, R417A, R422D and R422A gases, respectively.
Katırcıoğlu et al. [14]	R22, R417A, R438A	Experimental/ Heat pump	Using a new method of infrared image analysis, R438A was found to perform closer to R22 than R417A.

Table 1. *Cont.*

Reference	Refrigerant	Approach/System	Conclusions
Rocca and Panno [15]	R22, R417A, R422A, R422D	Experimental/ Heat pump	Although the gases used in the study could be used without oil change in the system, they did not provide better performance than R22.
Aprea et al. [16]	R22, R417A	Experimental/ Vapour compression refrigeration plant	In his study with R417A refrigerant, it was reported that R22 performed better, but R417A could be a long-term alternative in terms of being suitable for existing systems and being environmentally friendly. It was also found that the amount of exergy lost was 14% higher when R407C was used instead of R22.
Oruç and Devecioğlu [17]	R22, R417A, R424A	Experimental/ Heat pump	The COP value of R22 was found to be 17–23% and 4–14% larger than R417A and R424A, respectively.
Deymi-Dashtebayaz et al. [18]	R22, R417A	Experimental/ Split air conditioner	It is demonstrated that R22 and R417A have energy efficiency ratios of 2.48 and 2.41, respectively, and that their maximal energy efficiencies are around 7.3% and 7%.
Torrella et al. [19]	R22, R417A, R422D	Experimental/ Water cooler	It has been demonstrated that there will be a minor decrease in the system's cooling capacity if R22 is swapped out with R417A or R422D.
Shaik and Babu [20]	R407C, R1270, R290, RE170, R134a...	Analytical/ Heat pump	The COP value for the refrigerant with a blend of R134a/R1270/RE170 (based on a mass percentage of 55/37.5/7.5) is 5.35% higher than that of R22, R407C, and the four refrigerants studied.
Shaik and Babu [21]	Twenty-two refrigerants	Analytical/ Heat pump	The COP of the R134a/R1270/R290 triple blend (50%/5%/45% by mass percentage) was 2.01% higher than the COP of the studied R22 and twenty-two refrigerants.
Kalaiselvam and Saravanan [22]	R22, R417A and R407C	Experimental/ Heat pump	In a heat pump system using three types of scroll compressors, the exergy losses obtained for R22 were found to be 1% less than R417A and 1.5% less than R407C.The second law efficiency obtained in the case of using R22 was 50–55%, while this value was 48–52% for R407C and R417A refrigerants. It is reported that the use of R417A will be more efficient than the use of R407C to reduce exergy loss.
Wang et al. [23]	R22, R407C, R134a	Analytical/ Heat pump	The COP value obtained for R134a was found to be 3.3% and 8.6% higher than R22 and R407C, respectively. R134a was found to be more efficient than R407C compared to R22 for the new system.
Abdulqadir et al. [24]	R22, R407C	Experimental/ Heat pump	It was observed that the compressor outlet temperature of R407C was lower than R22. It is stated that the decreases in the evaporator and condenser parts of the system using R407C are less than R22. It is stated that R407C can be a good alternative due to its cooling effect and COP value being very close to R22.
Fatouh et al. [25]	R22, R407C	Experimental/Air conditioner	It was found that the inlet humidity provided an increase of 30% and 24.1% in the average COP for R22 and R407C, respectively. It is stated that R407C is a good alternative for R22. In terms of COP, the best performance was obtained when R22 was used compared to R407C.

Table 1. *Cont.*

Reference	Refrigerant	Approach/System	Conclusions
Lee et al. [26]	R22, R407C	Experimental/ Heat pump	The performance degradation due to the evaporator was found to be about twice as high as that of the condenser.
Aprea and Greco [27]	R22, R407C	Experimental/ Heat pump	It is stated that the exergetic efficiency obtained with R22 is greater than with R407C, and optimization should be made in the evaporator and condenser to increase the performance in the system using R407C.
Aprea and Greco, [28]	R22, R407C	Experimental/ Heat pump	It is claimed that the use of R22 gas improves compression performance since semi-hermetic compressors have higher isoentropic and volumetric efficiency than R407C.
Cabello et al. [29]	R22, R134a, R407C	Experimental/ Heat pump	The authors stated that the mass flow rate of refrigerant is significantly affected by the compression ratio and evaporation pressure.
Devotta et al. [30]	R22, R407C	Experimental/ Window type air conditioner	Under the same conditions, the cooling capacity of R407C was found to be 2.1–7.9% lower than that of R22.

A review of the literature presented in Table 1 reveals that most studies have focused on the effect of changing a single component (either the refrigerant or the equipment) in heat pumps. However, unlike the existing literature, this study has developed a combination that allows for the simultaneous evaluation of the refrigerant, the heat pump's core components, and the system operating conditions. This is because a heat pump's performance is significantly dependent on the simultaneous interaction between the evaporator and heat exchanger types and the refrigerant. Therefore, this study aims to fill the gap in the literature regarding multi-objective optimization by developing an analytical modeling approach that allows for the joint analysis of these three parameters.

In engineering applications related to meeting energy needs, modeling and simulation studies are utilized to eliminate system setup costs. In recent years, numerous modeling and optimization studies have been conducted in the literature to ensure that energy conversion is achieved both more efficiently and prior to implementation, with the aim of managing and reducing environmental impacts [31–40].

In the present study, the optimum operating conditions of the heat pump system were determined by the Taguchi analysis method by using R417A and R407C zeotropic gas mixtures as an alternative to R22. Then, using the data obtained, the COP and exergetic efficiency of the system at the optimum operating conditions were determined. The Taguchi method is a method used to determine the degree of influence of the factors affecting the process [41–43]. With this method, which determines the optimum operating parameters required to determine the performance of these factors, both the number of experiments is reduced, and the variability is aimed to be minimized. Among the controllable and uncontrollable parameters affecting the process, eliminating or reducing the negative effects of uncontrollable parameters may require very high costs. For this reason, it would be more accurate to use the controllable ones classified as control, correction, and ineffective parameters [44,45]. A product and process design developed by this method will reduce both production and the lifetime cost of the product [46]. In addition, Taguchi method analysis results will be useful since it is possible to provide the optimum working conditions determined in the laboratory in real application areas. While there are studies using the Taguchi method for engineering applications [47–56] and heat pump applications [57–64] and fewer studies using the Taguchi method in terms of energy analysis in heat pumps. For

this reason, the present study also aims to employ an analytical method in the experimental investigation of heat pump efficiency in terms of energy and exergy.

In a study by Xin and colleagues [65], which can serve as an example of heat pump research utilizing the Taguchi method, the complexity of dynamic energy matching in a multi-source heat pump was investigated. They combined the Taguchi method with the entropy weighting method to implement an orthogonal design for four control factors. Specifically, to ensure the dynamic prioritization and coordination of heterogeneous heat sources, they developed a new Taguchi-entropy weighting collaborative methodology.

In an experimental study conducted by Zamen and colleagues [66] on an innovative desalination system utilizing a water-source heat pump, the Taguchi method was employed to identify the optimal conditions for maximum efficiency at high salinity levels.

In another study conducted by Mołczan and colleagues [67], the Taguchi method was employed to achieve the unit's optimal energy efficiency and minimize drying time by utilizing a heat pump to supply heat to the drying chamber. The purpose of the simulation model used was not only to determine the values at which the operating parameters are optimized but also to facilitate the selection of system components.

As an example of energy and exergy studies conducted using the Taguchi method in heat pump systems, the studies by Çomaklı et al. [63,64] analyzed only the system's operating condition parameters (mixing concentrations, source temperature, cooling water flow rate, and air flow rate in the cooling tower). In contrast, the present study experimentally investigates the effects of the system's basic component types on performance coefficients and exergetic efficiency values.

The present study differs from previous optimization studies on heat pump systems in the literature in that it enables the examination of changes in system performance under different refrigerants and operating conditions within a system where various types of heat pump components can be connected to a simple heat pump system to operate independently of one another. The aim of this method is to guide studies that can identify the most efficient system components and evaluate multiple factors simultaneously. In short, unlike heat pump optimization studies in the literature, it enables the testing of the optimal configurations for both the refrigerant and the heat pump's basic components (the evaporator and the superheating cooling unit), as well as the heat pump operating conditions (condenser and evaporator flow rates), all within the same model. Following the same logic, this study could pave the way for new research where similar variations can be applied to other fundamental system components, such as the condenser, compressor, and expansion valve. Thus, the aim of this study is to serve as a model case where experimental results obtained under laboratory conditions can guide industrial applications.

In accordance with the objectives outlined above ın this study, a modified heat pump system was designed for use in cold climate regions for heating purposes, in which the types of system components, such as the evaporator and heat exchanger, were changed. In a system operating with R22, the effect of using alternative refrigerants on the system's COP and exergy efficiency was investigated.

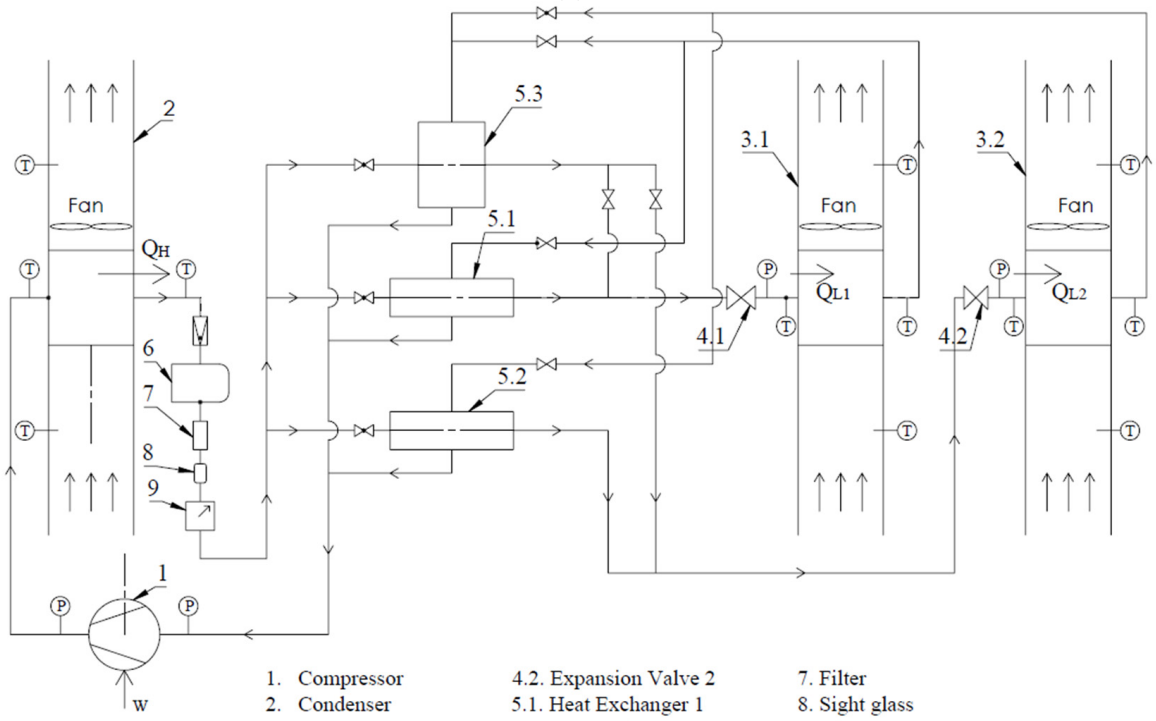
This study aims to determine the most efficient system performance when R417A and R407C gases are used as alternatives in a heat pump system operating with R22 gas, where two types of evaporators and two types of heat exchangers can be operated separately using the Taguchi method. The contribution of this study to the literature is that it allows for the testing of gases that can be used instead of R22, whose use is restricted, in an experimental heat pump system with different types of heat pump basic elements at flow rates. Using the Taguchi method, it also allows for the determination of the most efficient system performance conditions with fewer experiments in a modified heat pump system.

2. Material Method

The experimental setup of the heat pump operating according to the air-air operating cycle used in this study is shown in Figure 1a,b. The system consists of a 2.8 HP compressor, plate-fin air-cooled condenser, two different types of plate-fin air-cooled evaporators, a thermostatic expansion valve, horizontal and vertical heat exchangers, a gas flow meter, sight glass, dryer, oil separator, and auxiliary equipment.



(**a**)



(**b**)

Figure 1. (**a**) Heat pump experimental setup. (**b**) Heat pump experimental setup schematic representation.

The temperature and pressure of the working fluid were measured using a calibrated multi-channel digital temperature controller by means of T-type thermocouples placed at the inlet and outlet of the compressor, condenser, and evaporator, as shown in Figure 1b. Pressures were measured with four Bourdon-type manometers placed at the inlet and outlet of the basic elements. The current, voltage, and power factor values drawn by the compressor were determined with the digital multimeter used in the system. Using the results obtained, it was calculated how much power was supplied to the compressor. The amount of refrigerant and its mixture was measured with a sensitive digital scale and charged to the system. In order to create different ambient conditions, 5-stage electric resistances were added to the air inlet parts of the condenser and evaporators, and one speed control device (dimmer) was added to the fans. The air inlet temperatures of the condenser and evaporator were changed by operating the resistances at different levels. The airflow rates of the condenser and evaporator were also changed with the speed controllers.

Before starting the experiments, the system was loaded with refrigerant. Firstly, R22 gas was loaded into the system, and the temperature and pressure values taken from the points shown in Figure 1 were checked. It was observed that the data obtained in 20 min when the steady-state conditions were provided in the study stabilized. During the stabilization period, raw data were obtained by measuring pressures from manometers, temperatures from thermocouples, flow rate from gas flow meters, air flow rate from flow meters, current entering the compressor, volts, and power factor from digital multimeters. After it was determined that the measurement values on the system were taken correctly, the refrigerant was drained from the system. The experiments continued with the new gases to be investigated, R417A and R407C zeotropic mixture gases. The charging of the R417A and R407C refrigerants into the system was completed when the pressure gauges reached the lower and upper pressure values corresponding to the heat pump's operating range. Using this method, the heat pump system was charged with R417A refrigerant at approximately 12% less than R22 and R407C refrigerant at the same amount as R22.

Table 2 shows the basic properties of the refrigerants used. Table 3 shows the environmental properties of R22, R407C, and R417A. ODP values are a measure of the potential of other refrigerants to deplete stratospheric ozone compared to R11 refrigerant, given an ODP value of 1. Global warming potential (GWP) is a value describing the ability to harvest radiant energy compared to R11 and CO_2.

Table 2. Thermophysical properties of refrigerants used in the experiments [10].

Refrigerant	R22	R407C	R417A
Molar Mass (g/mol)	86.48	106.75	86.20
Boiling Temperature (°C)	−40.80	−39.12	−43.80
Critical Temperature (°C)	96.15	87.04	86.05
Critical Pressure (kPa)	4980	4036	4630

In this study, different refrigerants and flow rates (evaporator and condenser air flow rates) as well as both evaporator type and heat exchanger type parameters were tested on the same system with Taguchi analysis. Thus, the system elements that increase the heat pump system performance and the optimum operating conditions were tested in the same analysis.

For this purpose, the properties of two different types of evaporators included in the system are given in Tables 4 and 5. Two types of air evaporators were used in the experimental setup. One of the evaporators has an 8 mm lamella interval, and the other

has a 6 mm lamella interval. The properties of evaporators with a 6 mm lamella interval and an 8 mm lamella interval are given in Table 4. The reasons for using air-cooled evaporators are that they are simple, have low operating costs, and can be used in all kinds of cooling applications.

Table 3. Environmental characteristics of refrigerants [8].

Group	**HCFC**	**Zeotropic Mixtures**	
Refrigerant	R22	R407C	R417A
Chemical Formula	$CHCLF_2$	0.23R32/0.25R125/0.52R134a	0.466R125/0.5R134a/0.034R600
ODP	0.055	0	0
GWP (R11 = 1)	0.034	0.29. . .0.37	-
GWP (CO_2 = 1)	1900	1610	2300

Table 4. Properties of the evaporator with 6 and 8 mm lamella intervals used in the experimental setup.

Model	**6 GNE 40.1.5**	**8 GNE 40.1.5**
Capacity	4600 Watt	4000 Watt
Heat Transfer Surface Area	20.8 m^2	16.1 m^2
Pipe Volume	5.7 dm^3	5.7 dm^3
Number of Fans	1	1
Fan Diameter	400 mm	400 mm
Fan Flow Rate	3300 m^3/h	3500 m^3/h
Fluid Inlet Connection	12 mm	12 mm
Fluid Outlet Connection	22 mm	22 mm

Table 5. Vertical heat exchanger specifications.

Model	**SLA.E. 30B.16.10.2.5**
Refrigerant Type	HCFC-HFC-CFC
Capacity	2.5 lt
Max Working Pressure	30 Bar
Test Pressure	43 Bar
Operating Temperature	Min.: −20 °C/ Maks.: +130 °C
(1) Evaporator Arrival (Heat Exchanger Inlet)	5/8″ ODS
(2) Compressor Outlet (Heat Exchanger Outlet)	5/8″ ODS
(6) Coming from Condenser (Heat Exchanger Inlet)	3/8″ ODS
(7) Return to Expansion Valve (Heat Exchanger outlet)	3/8″ ODS

Two types of heat exchangers were used in the experimental setup to heat the refrigerant coming out of the evaporator before entering the compressor and to cool the refrigerant coming out of the condenser before entering the expansion valve. These are named as a horizontal heat exchanger and a vertical heat exchanger. The vertical heat exchanger is shown in Figure 2 [68], and its specifications are given in Table 5 [68].

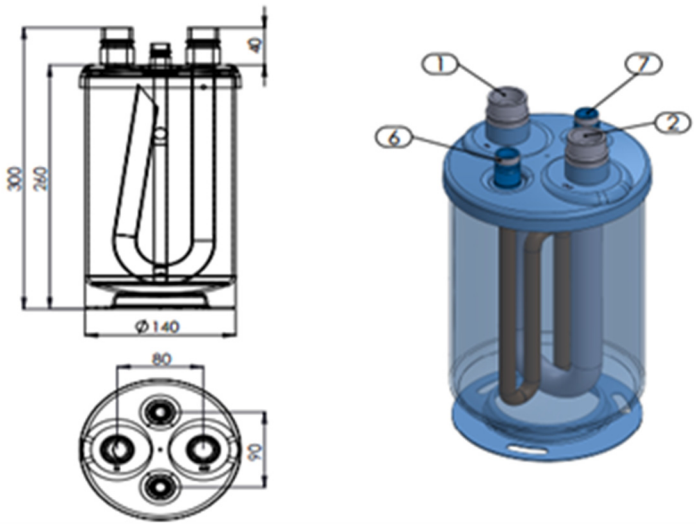


Figure 2. Vertical heat exchanger.

The horizontal heat exchanger consists of two intertwined copper tubes. The vapor-phase fluid from the evaporator passes through the inner copper tube, and the condensed fluid from the condenser passes through the inner part of the outer tube. The vapor-phase fluid leaving the evaporator heats up a little before going to the compressor, while the condensed fluid leaving the condenser and going to the expansion valve cools down a little. The horizontal heat exchanger is given in Figure 3.

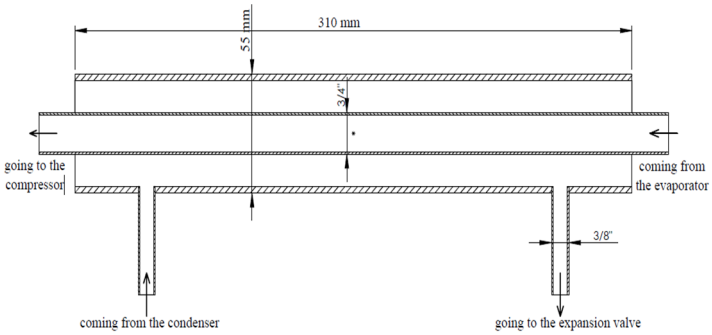


Figure 3. Horizontal heat exchanger.

Heat removed by the condenser:

$$\dot{Q}_{kon} = \dot{m}_{ref} \left(h_{con,out} - h_{con,in}\right) \quad (1)$$

Heat absorbed by the evaporator:

$$\dot{Q}_{ev} = \dot{m}_{ref} \left(h_{ev,in} - h_{ev,out}\right) \quad (2)$$

Input power to the compressor:

$$\dot{W}_{comp} = \sqrt{3}.Cos\varphi.U.I \quad (3)$$

where U, I, and Cosφ are voltage (V), current (A), and power factor, respectively. Coefficient of performance of the heat pump,

$$COP = \frac{\dot{Q}_{kon}}{\dot{W}_{comp}} \quad (4)$$

Exergetic efficiency is expressed as the ratio of the exergy taken or desired to be taken from a system to the exergy given to the system. The exergetic efficiency of a heat pump is denoted by η_{ex} [69,70].

$$\eta_{ex} = \frac{\sum \Delta \dot{E}_{x,ç}}{\sum \Delta \dot{E}_{x,g}} \quad (5)$$

Based on the formula,

$$\eta_{ex} = \frac{\dot{Q}_{kon} - T_0 \dot{m}_{con,air} c_{p_a} \ln\left(T_{con.air,out}/T_{con.air,input}\right)}{\dot{W}_{comp} + \dot{Q}_{eva} - T_0 . \dot{m}_{ev,air} c_{p_a} \ln\left(T_{ev.air,input}/T_{ev.air,out}\right)} \quad (6)$$

calculated with the formula above.

COP: Coefficient of performance
$\eta_{ex:}$ Exergetic efficiency
$\dot{m}_{ref}$: Mass flow rate of refrigerant (kJ/kg K)
$h_{con,out}$: Specific enthalpy of refrigerant leaving the condenser (kJ/kg)
$h_{con,in}$: Specific enthalpy of refrigerant entering the condenser (kJ/kg)
$h_{ev,in}$: Specific enthalpy of inlet refrigerant at evaporator (kJ/kg)
$h_{ev,out}$: Specific enthalpy of outlet refrigerant at evaporator (kJ/kg)
$\dot{E}_{x,ç}$: Total exergy transfer entering the system
$\dot{E}_{x,g}$: Total exergy output from the system
$\dot{Q}_{con}$: Heat given off to air from condenser (kW)
T_0: Ambient temperature (K)
$\dot{m}_{con,air}$: Mass flow rate of air passing through the condenser (kg/s)
c_{p_a}: Specific heat of air (kJ/kg K)
$T_{con.air,out}$: Temperature of air leaving the condenser (K)
$T_{con.air,input}$: Temperature of air entering the condenser (K)
$\dot{W}_{comp}$: Power of compressor (kW)
$\dot{Q}_{ev}$: Heat taken from air in evaporator (kW)
$\dot{m}_{ev,air}$: Mass flow rate of air passing through the evaporator (kg/s)
$T_{ev.air,input}$: Temperature of air entering the evaporator (K)
$T_{ev.air,out}$: Air temperature leaving the evaporator (K)

In this study, the optimum operating parameters of the system were determined from the variance analysis tables generated by using the Taguchi method. For this purpose, an experimental plan was prepared according to the Taguchi method under constant ambient temperatures (condenser inlet temperature of 19 °C and evaporator inlet temperature of 15 °C). Each experiment mentioned in the table was repeated 6 times, and calculations were made by considering the average of the results.

2.1. Experimental Plan for Optimization

Achieving robustness in the design of a process is important for a variety of purposes, since variability is inherent in all processes. Such performance measurements, known as signal-to-noise (S/N) ratios, are used to identify the ideal settings of controllable parameters in the Taguchi approach, which was created to design products and processes that are not susceptible to uncontrollable factors [71]. For this purpose, an analysis of variance table is created to determine the percentage of influence of factors affecting a product or process. Thus, it is easier to optimize the results obtained. In this method, using orthogonal arrays, the effect of the maximum number of effective parameters on the product is investigated with the minimum number of experiments.

Each orthogonal array used in the Taguchi method is uniquely identified by a code, making it possible to select suitable arrays depending on the number of parameters and stages.

In the code $L_n(m^k)$, n is the number of rows, m is the number of parameter levels, and k is the number of parameters.

Inner and outer arrays are the two experimental designs used in the Taguchi experimental process. The inner array contains all of the control factors. The outer array is used to evaluate all noise factors. Different combinations of noise factors in the outer array are tested against every combination of factor-level control factors in the inner array. The "signal-to-noise" ratio is then examined in order to identify the ideal parameter settings. The signal-to-noise ratio, or S/N ratio, is a performance metric used in the Taguchi technique.

Depending on the intended performance response, there are three common forms of S/N ratios.

- Smaller is better (in order to minimize the system's reaction).

  S/N can be calculated as given below

$$S/N = -10 \log\left(\frac{1}{n}\sum_{i=1}^{n} y_i^2\right) \quad (7)$$

- Nominal value is best (to reduce variability around a target).

  S/N can be calculated as given below

$$S/N = -10 \log\left(\frac{1}{n}\sum_{i=1}^{n} (y_i - y_o)^2\right) \quad (8)$$

- Bigger is better (to make the system response as large as possible).

  S/N can be calculated as follows:

$$S/N = -10 \log\left(\frac{1}{n}\sum_{i=1}^{n} \frac{1}{Y_i^2}\right) \quad (9)$$

where n is the number of repetitions for a combination of experiments and y_i is the performance value of the i-th trial [72].

It is expected that the optimum working conditions of the system obtained by the Taguchi method will always give the same value with minimum difference, or directly in different times and in different working environments. In other words, if the optimization is capable of controlling the intended result or the minimum level of variability around it, it will have achieved the desired precision. According to the Taguchi method, an optimization criterion that satisfies these properties will also satisfy the performance statistic (signal-to-noise). Therefore, the optimization criterion developed for the bigger-is-better case, performance statistics will be preferred as the optimization criterion. In order to reduce the number of experiments and the cost of the product or process, if the experiment corresponding to the optimum operating conditions of the experimental design model used has not been performed during the study process, the performance value corresponding to the optimum conditions can be estimated based on the balanced property of orthogonal arrays. For this purpose

$$Y_i = \mu + X_i + e_i \quad (10)$$

The additive model expressed by Equation (10) is utilized. Since Equation (10) is a point estimate based on the data obtained from the experimental results, a confidence

interval must be determined to determine whether the results of the verification experiment are significant. The confidence interval at the selected error level is

$$Y_i \pm \sqrt{F_{\alpha;1;SD_{MS_e}} \times MS_e \times \left[\frac{1+m}{N} + \frac{1}{n_t}\right]} \quad (11)$$

is calculated from the formula. In the formula, N is the total number of experiments, and m is Total degrees of freedom of the parameters used in the estimation, n_i refers to the number of repetitions in the validation experiment [44].

In this study, since a two-level parameter and seven three-level parameters will be examined, the L18 (21 × 37) orthogonal array was selected as the experimental design best suited to these conditions. Since preliminary tests conducted prior to the study indicated that the interactions among the other parameters could be neglected, only the interaction between A (the parameter placed in the first column) and B (the parameter placed in the second column) was examined. The validity of this assumption was verified through validation experiments conducted under optimal conditions.

In this study, the optimum operating conditions of 3 different refrigerants were tried to be determined by the Taguchi Method by using different condenser flow rates, different evaporator flow rates, different evaporators, and different heat exchangers by using a vapor compression heat pump experimental setup. According to the Taguchi method, the L_{18} ($2^1.3^7$) experiment plan was applied. According to the L_{18} experimental plan, experiments should be carried out according to the 3-level change of 5 parameters, while 2 parameters were studied as 2-level and 3 parameters were studied as 3-level in this study. Under normal conditions, 3 × 3 × 3 × 2 × 2 = 108 experiments should be performed in order to find the optimum working conditions in a system with 3 parameters at 3 levels and 2 parameters at 2 levels, while optimum working conditions were determined by performing 18 experiments with the Taguchi method.

2.2. Experimental Uncertainties

Using the estimation method of Kline and McClintock [73], as well as the individual contributions of each physical property to the uncertainties of the COP and exergy efficiency, are summarized in Table 6.

Table 6. Uncertainties in the values of the relevant variables.

Variables	Uncertainty (%)
Temperature (T)	2.5
Pressure (P)	1.6
Voltage(V)	1.7
Current (I)	1.7
Power factor (Cos ϕ)	1.7
Mass flow rate (m_r)	1.3

3. Results Obtained by Taguchi Method

The parameters and levels examined in the experiments prepared according to the Taguchi method are given in Table 7, and the experimental plan is given in Table 8.

Table 7. Parameters and levels analysed in the experiments.

Parameter Code	Parameter Name	1st Level	2nd Level	3rd Level
A	Evaporator type	6 mm lamella ınterval	8 mm lamella ınterval	-
B	Refrigerant type	R22	R417 A	R407 C
C	Evaporator air flow (kg/s)	0.63	0.92	1.11
D	Condenser air flow (kg/s)	0.51	0.77	0.89
E	Heat exchanger type	Horizontal	Vertical	-

Table 8. L_{18} ($2^1.3^7$) Experimental plan.

Experiment No	Evaporator Type	Refrigerant Type	Evaporator Air Flow Rate	Condenser Air Flow Rate	Heat Exchanger Type
	A	B	C	D	E
1	1	1	1	1	1
2	1	1	2	2	2
3	1	1	3	3	2′
4	1	2	1	1	2
5	1	2	2	2	2′
6	1	2	3	3	1
7	1	3	1	2	1
8	1	3	2	3	2
9	1	3	3	1	2′
10	2	1	1	3	2′
11	2	1	2	1	1
12	2	1	3	2	2
13	2	2	1	2	2′
14	2	2	2	3	1
15	2	2	3	1	2
16	2	3	1	3	2
17	2	3	2	1	2′
18	2	3	3	2	1

Using the COP and exergetic efficiency data obtained from Table 8, analysis of variance tables were created to determine the optimum operating conditions of the system. The optimum operating conditions were determined by making use of the variance analysis tables.

3.1. Variance Analysis Results According to Raw COP Data

Analysis of variance was performed on the raw data to determine whether the parameters are effective or not. From the variance analysis results prepared by using raw COP data, it is seen that evaporator type is effective at the 5% level, refrigerant parameter is effective at the 1% level, condenser air flow rate is effective at the 1% level, and heat exchanger type is effective at the 1% level.

As indicated in Table 7, parameter A is the evaporator type, B is the refrigerant type, C is the evaporator air flow rate, D is the condenser air flow rate, and E is the heat exchanger type. The effects of these 5 parameters on the raw COP values are given in Figures 4, 5, 6, 7, and 8, respectively.

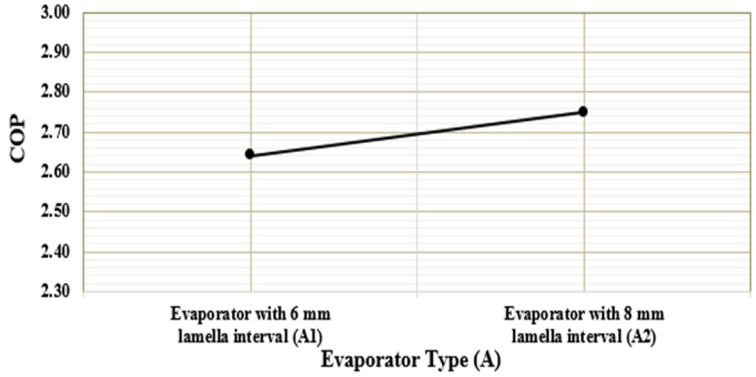


Figure 4. Effect of evaporator type on COP.

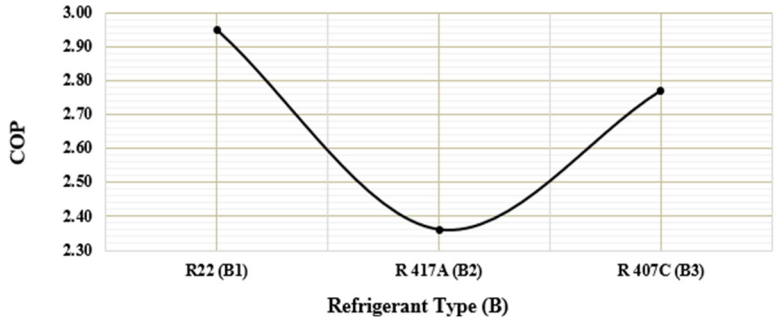


Figure 5. Effect of refrigerant type on COP.

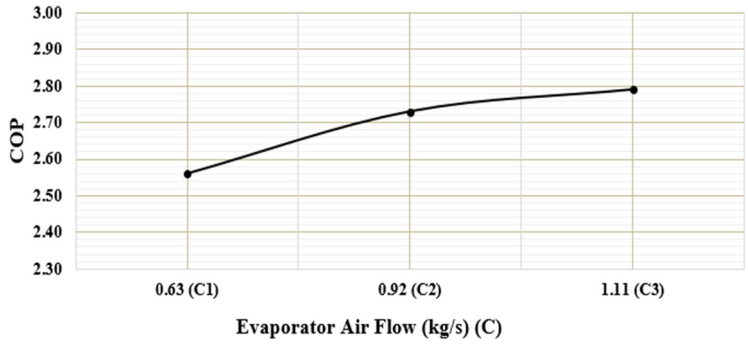


Figure 6. Effect of evaporator air flow rate on COP.

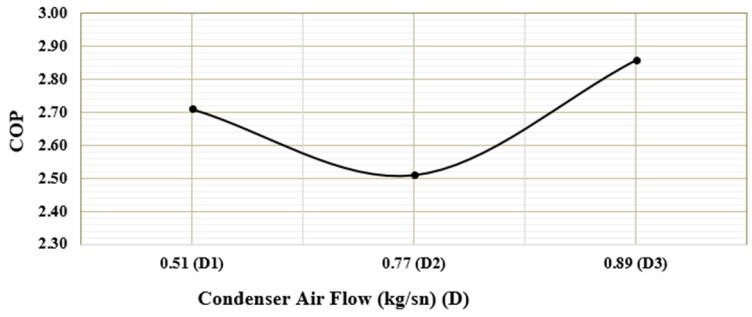


Figure 7. Effect of condenser air flow rate on COP.

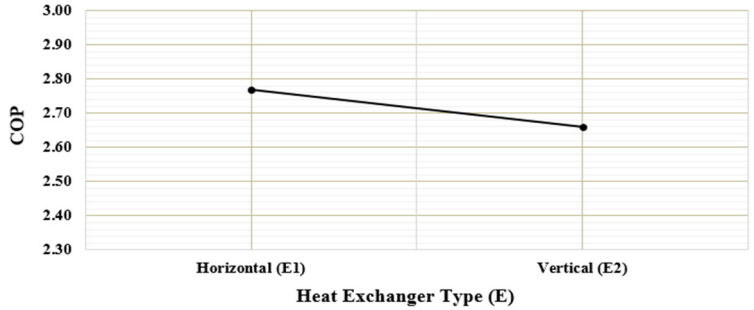


Figure 8. Effect of heat exchanger type on COP.

As seen in Figures 4–8, the optimum operating conditions obtained from raw COP data are determined as **A_2 B_1 C_3 D_3 E_1**. Optimum operating conditions (COP—for raw data) are A_2: Evaporator Type: 8 mm lamella ınterval, B_1: Refrigerant: R22, C_3: Evaporator air flow rate: 1.11 kg/s, D_3: Condenser air flow rate: 0.89 kg/s, E_1: Heat exchanger type: Horizontal.

3.2. Analysis of Variance Results Based on Converted COP Data

As a result of the analysis of variance using the (S/N) data values obtained from the conversion of COPs using Equation (7), the refrigerant parameter is effective at 1%, and the condenser air flow rate parameter is effective at 5%. Other parameters are not effective. The effects of these 5 parameters on the S/N data are given in Figures 9–13.

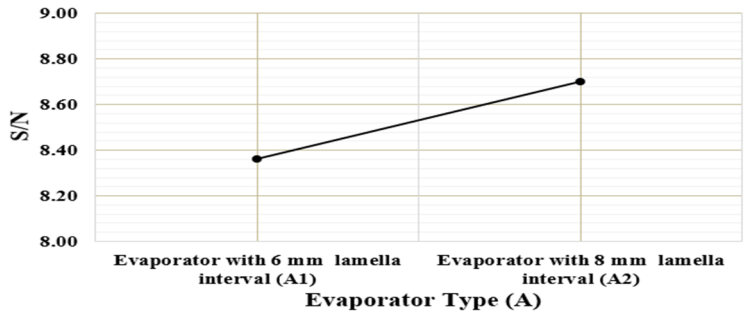


Figure 9. Effect of evaporator type on S/N.

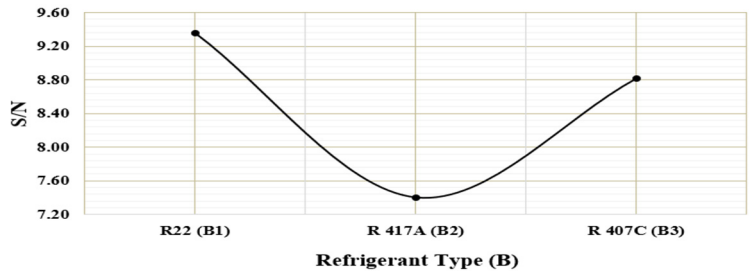


Figure 10. Effect of refrigerant type on S/N.

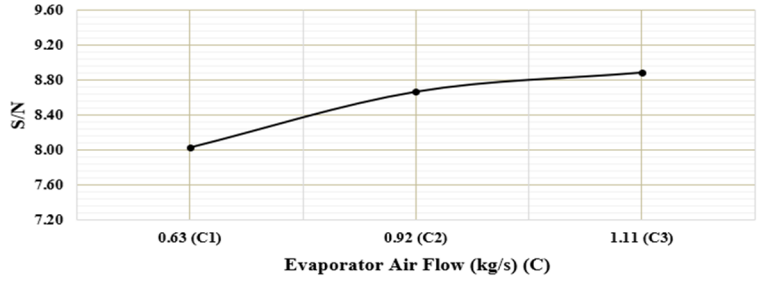


Figure 11. Effect of evaporator air flow rate on S/N.

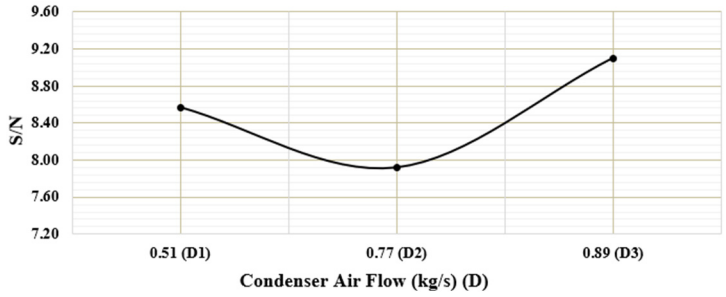


Figure 12. Effect of condenser air flow rate on S/N.

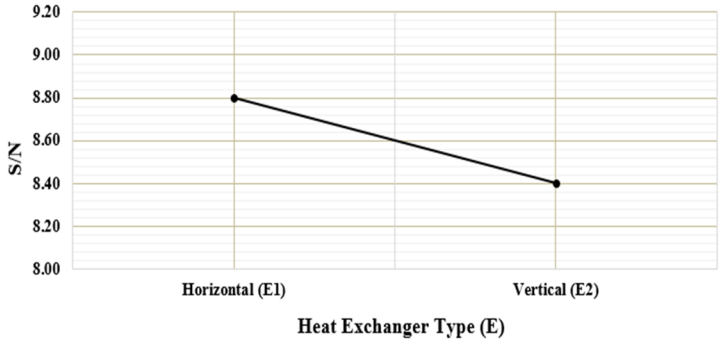


Figure 13. Effect of heat exchanger type on S/N.

As seen in Figures 9–13, the optimum operating conditions obtained from the converted COP (S/N) data are determined as $\mathbf{A_2B_1C_3D_3E_1}$ or $\mathbf{B_1D_3}$. Optimum operating conditions (S/N—for converted data) are B_1: Refrigerant: 100% R22, D_3: Condenser air flow rate: 0.89 kg/s.

As shown in Figures 5 and 10, the Taguchi analysis revealed that the raw COP value of R22 refrigerant is 25% higher than that of R417A and 6.5% higher than that of R407C, and, based on the data obtained by converting the COPs, 26.48% and 6.12% higher, respectively.

Consequently, the Taguchi analysis revealed that the raw COP value of R407C is 17.37% higher than that of R417A and 19.18% higher compared to the data values obtained by converting the COPs, due to the system's resistance to noise factors.

As shown in Figures 4 and 9, when looking at Tables 4 and 5, it is found that the heat convection coefficient of the evaporator with an 8 mm lamella interval is greater than that of the evaporator with a 6 mm lamella interval, based on calculations using Newton's cooling law, when both evaporators experience the same temperature difference (ΔT). Therefore, the suitability of the evaporator with an 8 mm lamella interval in terms of optimum conditions compared to the evaporator with a 6 mm lamella interval in the optimum operating conditions obtained according to the Taguchi method was also confirmed by the analysis of variance.

Analytically, using the thermal capacity and heat transfer surface area of the unit as listed in the evaporator catalog specifications—for example, when a temperature difference (ΔT) of 10 K is taken as a reference—it can be determined that the heat transfer coefficient of an evaporator with an 8 mm fin spacing is approximately 15% higher than that of an evaporator with a 6 mm fin spacing.

Furthermore, the fact that the fan capacity of the evaporator with an 8 mm fin spacing is 200 m^3/h greater than that of the evaporator with a 6 mm fin spacing, it is believed that the evaporator in question offers advantages not only in terms of heat capacity but also in terms of fan power, and that the 8 mm fin-spaced evaporator played a role in the higher heat transfer observed in the experiments.

As shown in Figures 8 and 13, according to the results obtained from the Taguchi method, when the effects of heat exchangers on the performance of the system are analyzed comparatively, it is seen that the COPs are higher when horizontal heat exchangers are used than when vertical heat exchangers are used. However, the volumetric capacity of the vertical heat exchanger is higher than that of the horizontal heat exchanger. Therefore, although the volumetric capacity of the vertical heat exchanger was 3.33 times greater than the volumetric capacity of the horizontal heat exchanger, the horizontal heat exchanger was more efficient. Thus, it was determined that this result was obtained due to the higher surface area in contact between the refrigerants that provide superheat cooling to the heat pump system in the horizontal heat exchanger. It is evaluated that the higher performance values of the system in the case of using horizontal heat exchangers are due to the structure of the heat exchangers.

3.3. Analysis Result of Raw COP and Converted COP Data

The optimum operating conditions for raw COP data and converted COP (S/N) data are given in Table 9.

Table 9. Optimum operating conditions table created from raw COP data and converted COP (S/N) data results.

Parameter	Impacts on Average Raw COP	Effects on Transformed Data (S/N)	Optimum Working Conditions
A: Evaporator type	(2) $^{+}$	-	2: Evaporator with 8 mm lamella interval
B: Refrigerant	(1) *	(1) *	1: R22 Refrigerant
C: Evaporator air flow	(3) *	-	3: Evaporator air flow rate
D: Condenser air flow	(3) *	(3) $^{+}$	3: Condenser air flow rate
E: Heat exchanger type	(1) $^{+}$	-	1: Horizontal heat exchanger

* Effective parameters at 1% error level. $^{+}$ Effective parameters at 5% error level.

When examining the physical and statistical causes of the raw data and S/N results in the analysis of variance, while evaporator type A and heat exchanger type E produced a significant difference in the raw COP data, the disappearance of these effects in the S/N analysis indicates that the primary factors determining the system's resistance to noise factors are refrigerant type B and condenser flow rate D. Therefore, for industrial-scale applications where ambient temperature varies, $\mathbf{B_1\ D_3}$ will provide more stable operation.

3.4. Analysis of Variance Results According to Raw Exergetic Yield Data

Analysis of variance was performed on the raw exergetic efficiency data to determine the effectiveness of the parameters, and according to the analysis of variance table, only the condenser air flow rate was found to be effective. The effects of the 5 parameters on the raw exergetic efficiency (η_{ek}) are given in Figures 14, 15, 16, 17, and 18, respectively.

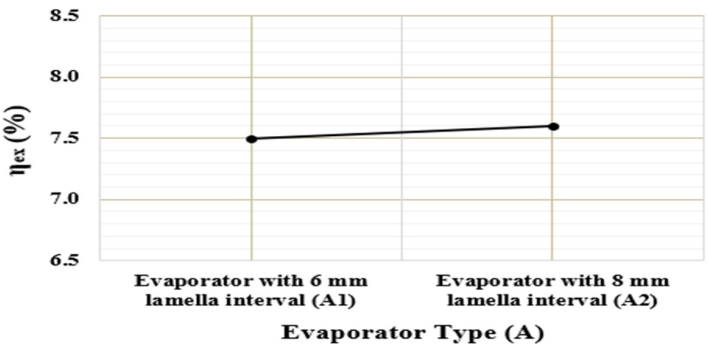


Figure 14. Effect of evaporator type on exergetic efficiency.

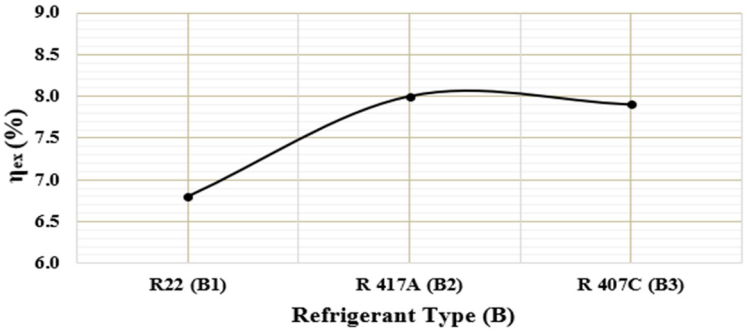


Figure 15. Effect of refrigerant type on exergetic efficiency.

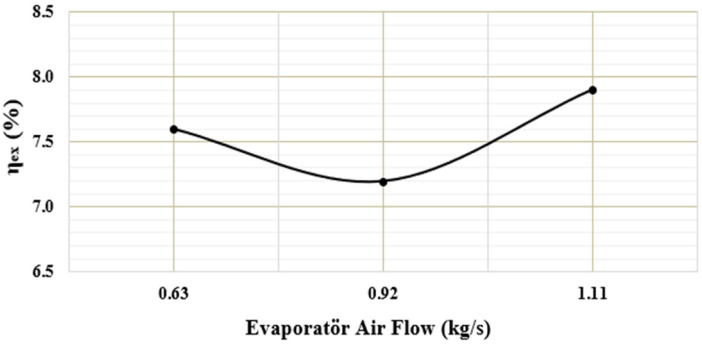


Figure 16. Effect of evaporator air flow rate on exergetic efficiency.

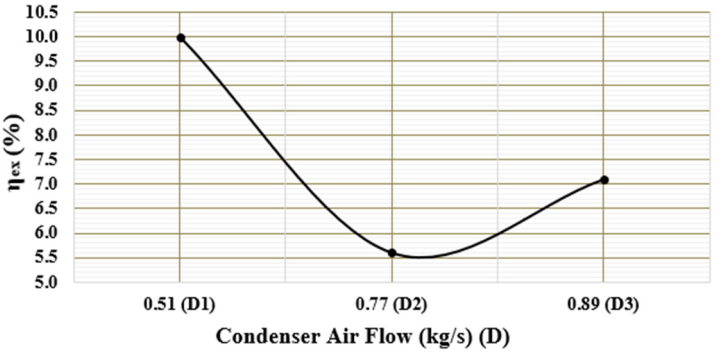


Figure 17. Effect of condenser air flow rate on exergetic efficiency.

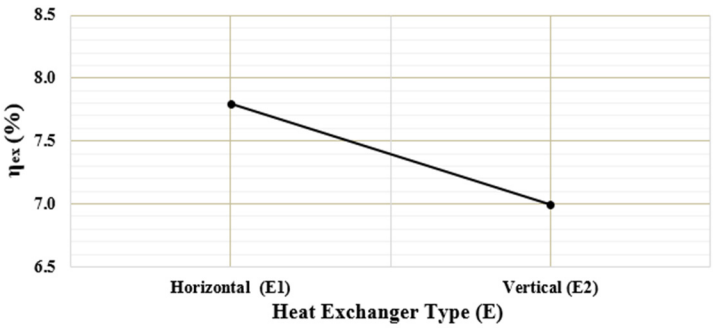


Figure 18. Effect of heat exchanger type on exergetic efficiency.

As seen in Figures 14–18, the optimum operating conditions obtained from the raw exergetic efficiency data were determined as $\mathbf{A_2B_2C_3D_1E_1}$ or $\mathbf{B_1D_1}$ or $\mathbf{D_1}$.

3.5. Analysis of Variance Results Based on Converted Exergetic Yield Data

Analysis of variance was performed on the converted exergetic efficiency data to determine the effectiveness of the parameters, and the effects of the 5 parameters on the converted exergetic efficiency (S/N) are given in Figures 19, 20, 21, 22, and 23, respectively.

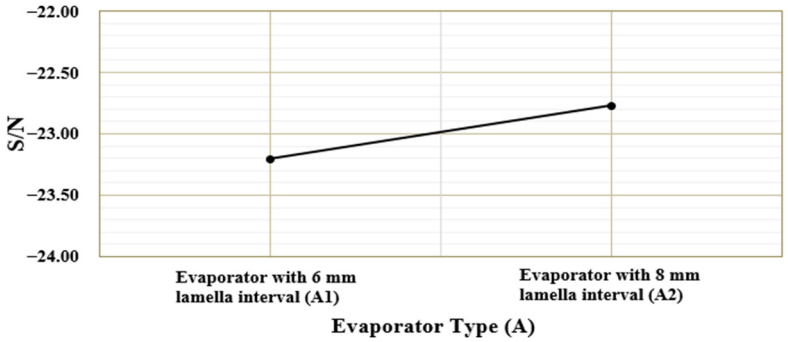


Figure 19. Effect of evaporator type on S/N.

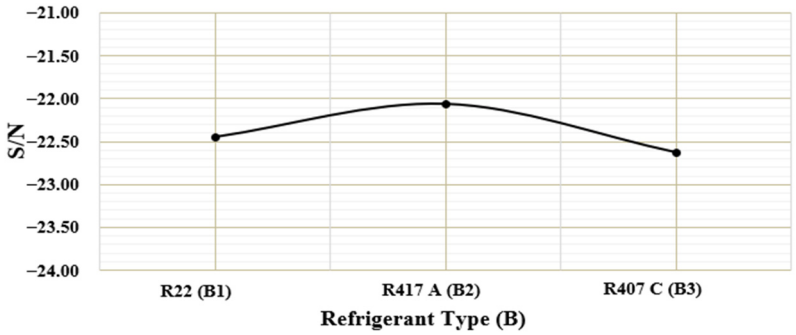


Figure 20. Effect of refrigerant type on S/N.

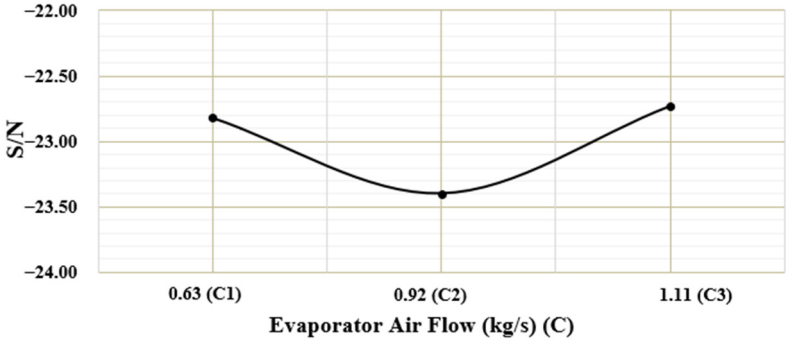


Figure 21. Effect of evaporator air flow rate on S/N.

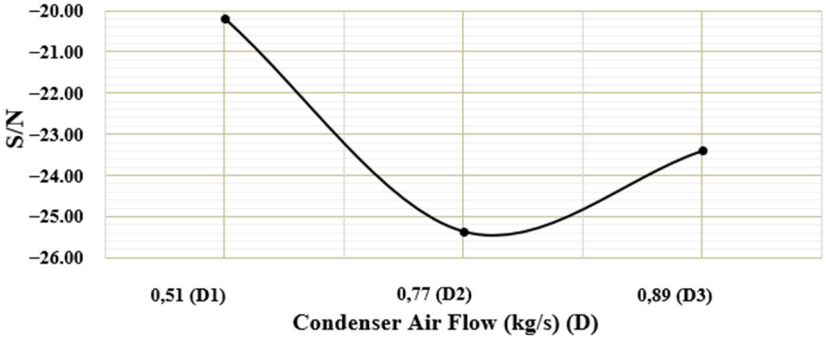


Figure 22. Effect of condenser air flow rate on S/N.

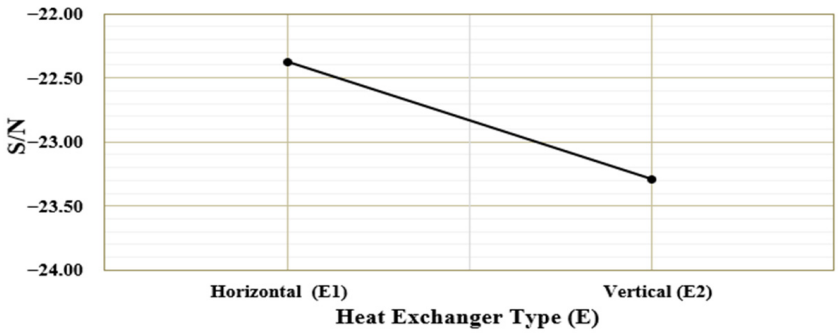


Figure 23. Effect of heat exchanger type on S/N.

As seen in Figures 19–23, the optimum operating conditions obtained from the converted exergetic efficiency data were determined as $\mathbf{A_2B_2C_3D_1E_1}$ or $\mathbf{B_2D_1}$ or $\mathbf{D_1}$.

As shown in Figure 15, the Taguchi analysis revealed that the raw exergetic efficiency of R417A gas is 17.64% higher than that of R22 and 16.17% higher than that of R407C. As shown in Table 10 below, which presents the raw and converted exergetic efficiency data and the resulting optimal operating conditions, R417A is indicated as the best refrigerant in terms of exergetic efficiency under optimal conditions.

Table 10. Table of optimum operating conditions based on exergetic efficiency raw data and transformed exergetic efficiency data results.

Parameter	Impact on Average	Impact on Variability	Optimum Working Conditions
A: Evaporator type	2	2	2: Evaporator with 8 mm lamella interval
B: Refrigerant	2	2	2: R417 Refrigerant
C: Evaporator air flow	3	3	3: Evaporator air flow rate
D: Condenser air flow	(1) *	(1) *	1: Condenser air flow rate
E: Heat exchanger type	1	1	1: Horizontal heat exchanger

* Effective parameters at 1% error level.

As shown in Figures 18 and 23, according to the results obtained from the Taguchi method, when the effects of heat exchangers on the exergetic efficiency of the system are analyzed comparatively, it is seen that the exergetic efficiency values are higher when horizontal heat exchangers are used than when vertical heat exchangers are used.

3.6. Raw Exergetic Efficiency and Converted Exergetic Efficiency Analysis Result

The optimum operating conditions for the raw exergetic efficiency data and converted exergetic efficiency data are given in Table 10.

The optimum operating conditions are determined as $\mathbf{D_1}$ when only the active parameter is considered. When other less efficient parameters are taken into account, it can be expressed as $\mathbf{A_2B_2C_3D_1E_1}$.

3.7. Result of Analysis of Raw Data (COP and Exergetic Efficiency) and Transformed Data (COP and Exergetic Efficiency)

The optimum operating conditions obtained from raw and transformed data are given in Table 11.

When Table 11 is examined, for COP, the optimum operating conditions $\mathbf{A_2B_1C_3D_3E_1}$ are obtained for an 8 lamella interval evaporator, R22 refrigerant, 1.11 kg/s evaporator air flow rate, 0.89 kg/s condenser air flow rate, and horizontal heat exchanger. For exergetic efficiency, $\mathbf{A_2B_2C_3D_1E_1}$ optimum operating conditions were obtained for 8 mm lamellar spaced evaporator, R417 refrigerant, 1.11 kg/s evaporator air flow rate, 0.51 kg/s condenser

air flow rate, horizontal heat exchanger. In addition, when the general optimum operating conditions obtained from the raw and transformed data of COP and exergetic efficiency are examined, general optimum conditions 1 and 2 are obtained as $\mathbf{A_2B_1C_3D_1E_1}$; and $\mathbf{A_2B_1C_3D_3E_1}$ respectively.

Table 11. Table of general optimum operating conditions obtained from raw and transformed data of COP and exergetic efficiency.

Parameter	COP Optimum Conditions	Exergetic Efficiency Optimum Conditions	General Optimum Conditions 1	General Optimum Conditions 2
A: Evaporator type	(2) $^{+}$	(2)	(2) $^{+}$	(2) $^{+}$
B: Refrigerant	(1) *	(2)	(1) *	(1) *
C: Evaporator air flow	(3) *	(3)	(3) *	(3) *
D: Condenser air flow	(3) *	(1) *	(1) *	(3) *
E: Heat exchanger type	(1) $^{+}$	(1)	(1) $^{+}$	(1) $^{+}$
COP values estimated to be obtained under optimum operating conditions			3.19	3.34
95% confidence intervals for optimum operating conditions (lower and upper limits of estimates)			2.938–3.442	3.088–3.592
Exergetic efficiency values estimated to be obtained under optimum operating conditions			9.6%	6.9%
Confidence limits at the 95% confidence level for optimum operating conditions (lower and upper limits of upper limits)			7.04–12.16	4.34–9.46

* Effective parameters at 1% error level. $^{+}$ Effective parameters at 5% error level.

Considering the results obtained from the Taguchi analysis, the key points to consider when selecting an evaporator and heat exchanger during the design of an industrial heat pump can be summarized as follows. When selecting heat exchangers—such as the condenser or evaporator, which are fundamental components of a heat pump—it may be necessary to choose among multiple models. In such cases, it has been determined that comparing the heat transfer coefficients of these components, which are used for heat transfer, and selecting the one with the higher heat transfer coefficient is the correct approach, as confirmed by the analysis results. To make this selection, the thermal capacity and heat transfer surface area of the devices to be selected, as listed in the product catalog, must be substituted into Newton's law of cooling equation to determine the heat transfer coefficients corresponding to a specific ΔT temperature difference. According to the analysis results, selecting a horizontal-type heat exchanger for the optimal configuration will also increase system efficiency. Considering the analysis results indicating that R407C gas can be preferred for system performance and R417A gas for exergetic efficiency over R22—which has an ODP value of 0.055 and a GWP value of 0.034, and is banned for use—will be beneficial for the industrial heat pump being designed. Thus, the analysis results obtained from experiments can be utilized in the design of an industrial system

4. Conclusions

In this article, the effects of using different types of evaporators with approximately equal capacity at different condenser and evaporator flow rates and horizontal and vertical-type heat exchangers as superheat/cooling units on system performance. Air-air-based heat pump systems using R22, R417A, and R407C as refrigerants were investigated by variance analysis.

Variance analysis tables were created for COP and exergetic efficiency by using the results of the experiments performed according to the experimental plan determined by the Taguchi analysis method. Using the variance analysis tables, 2 different optimum operating conditions were determined for the system. The first optimum operating condition is the heat pump operating system consisting of an evaporator with an 8 mm lamella interval, R22 refrigerant, a 1.11 kg/s evaporator air flow rate, a 0.51 kg/s condenser air flow rate, and a horizontal-type heat exchanger. The second optimum operating condition is the heat pump operating system consisting of an evaporator with 8 mm lamella interval, R22 refrigerant, 1.11 kg/s evaporator air flow rate, 0.89 kg/s condenser air flow rate, and a horizontal type heat exchanger.

In the first optimum operating conditions, the range of COP values calculated according to the Taguchi variance analysis table is 2.938 to 3.442, and the range of exergetic efficiency values is 7.04 to 12.616. The COP value found as a result of the experiment carried out under the specified conditions is 3.06, and the exergetic efficiency value is 11.63. In the second optimum operating condition, the range of COP values calculated according to the Taguchi variance analysis table is 3.008 to 3.595, and the range of exergetic efficiency values is 4.34 to 9.46. As a result of the experiment conducted under the specified conditions, the COP value is 3.42, and the exergetic efficiency value is 8.74.

The results of the verification experiments carried out in accordance with both optimum operating conditions determined according to Taguchi analysis were found to be within the confidence interval determined by the method. Thus, it was confirmed that the results of the experimental study were compatible with the variance analysis results.

The results of the study demonstrated that the evaporator with an 8 mm fin spacing is the optimal evaporator due to its higher heat transfer coefficient.

As a result, according to the results of the analysis, when the effects of the evaporator types on the performance of the system are analyzed comparatively, the efficiency of the system is more advantageous in terms of COP and exergetic efficiency when using 8 mm lamella interval evaporator than when using 6 mm lamella interval evaporator.

When using horizontal heat exchangers, it has been observed that the higher performance values of the system depend on the structure of the heat exchangers.

As a result of the Taguchi analysis, it was seen that although the performance of R417A and R407C gases tested as an alternative to R22 in the heat pump system was not better than R22, they could be used instead of R22 as an alternative refrigerant due to their close performance and better environmental effects.

It is also thought that it will be a guide for industrial-scale heat pump applications to be installed in real application areas, where the optimum operating conditions determined in the laboratory environment by utilizing the Taguchi method can be adapted.

This article is derived from Mehmet AKKOCA's Master's Thesis conducted under the supervision of Dr. Fadime ŞİMŞEK.

Author Contributions: Conceptualization, F.Ş.; Methodology, F.Ş.; Software, M.A.; Validation, M.A.; Formal analysis, F.Ş.; Investigation, M.A.; Data curation, M.A.; Writing—original draft, F.Ş.; Writing—review & editing, F.Ş.; Project administration, F.Ş. All authors have read and agreed to the published version of the manuscript.

Funding: This research received no external funding.

Data Availability Statement: The original contributions presented in this study are included in the article. Further inquiries can be directed to the corresponding author.

Conflicts of Interest: The authors declare no conflict of interest.

References

1. Dincer, I. Renewable energy and sustainable development: A crucial review. *Renew. Sustain. Energy Rev.* **2000**, *4*, 157–175. [CrossRef]
2. Wu, D.; Hu, B.; Wang, R. Vapor compression heat pumps with pure Low-GWP refrigerants. *Renew. Sustain. Energy Rev.* **2021**, *138*, 110571. [CrossRef]
3. United Nations Environmental Programme. *Montreal Protocol on Substances That Deplete the Ozone Layer; Final Act*; United Nations: New York, NY, USA, 1987.
4. Wei, F.; Wang, B.; Cui, M. Refrigerant screening method based on life cycle expense considering greenhouse gas emission for industrial heat pump. *Appl. Therm. Eng.* **2025**, *265*, 125643. [CrossRef]
5. Leggett, J. A guide to the Kyoto protocol: A treaty with potentially vital strategic implications for the renewables industry. *Renew. Sustain. Energy Rev.* **1998**, *2*, 345–351. [CrossRef]
6. Braga, C.H.M.; Martins, L.V.S.; Pabon, J.J.G.; Machado, L.; Duarte, W.M. Energetic, economic and environmental (3E) analysis of R290, R454C and R465A for drop-in split type air conditioning running on R22. *Case Stud. Therm. Eng.* **2025**, *69*, 105988. [CrossRef]
7. Aprea, C.; Mastrullo, R.; Renno, C. An analysis of the performances of a vapour compression plant working both as a water chiller and a heat pump using R22 and R417A. *Appl. Therm. Eng.* **2004**, *24*, 487–499. [CrossRef]
8. Sarbu, I. A review on substitution strategy of non-ecological refrigerants from vapour compression-based refrigeration, air-conditioning and heat pump systems. *Int. J. Refrig.* **2014**, *46*, 123–141. [CrossRef]
9. Fannou, J.L.C.; Rousseau, C.; Lamarche, L.; Kajl, S. A comparative performance study of a direct expansion geothermal evaporator using R410A and R407C as refrigerant alternatives to R22. *Appl. Therm. Eng.* **2015**, *82*, 306–317. [CrossRef]
10. Messineo, A.; Rocca, V.L.; Panno, G. On-site Experimental Study of HCFC-22 Substitution with HFCs Refrigerants. *Energy Procedia* **2012**, *14*, 32–38. [CrossRef]
11. Joudi, K.A.; Al-Amir, Q.R. Experimental Assessment of residential split type air-conditioning systems using alternative refrigerants to R-22 at high ambient temperatures. *Energy Convers. Manag.* **2014**, *86*, 496–506. [CrossRef]
12. Ergün, A.; Gürel, A.E.; Ceylan, İ. Performance Analysis of R438a and R417a Refrigerants as an Alternative to R22 in Commercial Cooling Systems. *Gazi Univ. J. Sci. Part C Desıgn Technol.* **2018**, *6*, 824–833. [CrossRef]
13. Cingiz, Z.; Katırcıoğlu, F.; Çay, Y.; Kolip, A. The Thermodynamic Analysis of the Refrigerants Alternative to R22 in the Vapor Compression Refrigeration System. *J. Polytech.* **2020**, *23*, 1205–1212.
14. Katırcıoğlu, F.; Cingiz, Z.; Çay, F.; Gürel, A.E.; Sarıdemir, S.; Kolip, A. Investigation of refrigeration system performance using infrared image processing techniques for R22 and its alternatives, R438A and R417A refrigerants. *Acad. Platf. J. Eng. Sci.* **2020**, *8*, 500–513.
15. Rocca, V.L.; Panno, G. Experimental performance evaluation of a vapour compression refrigerating plant when replacing R22 with alternative refrigerants. *Appl. Energy* **2011**, *88*, 2809–2815. [CrossRef]
16. Aprea, C.; Renno, C. Experimental comparison of R22 with R417A performance in a vapour compression refrigeration plant subjected toa cold store. *Energy Convers. Manag.* **2003**, *45*, 1807–1819.
17. Oruç, V.; Devecioğlu, A.G. Thermodynamic performance of air conditioners working with R417A and R424A as alternatives to R22. *Int. J. Refrig.* **2015**, *55*, 120–128. [CrossRef]
18. Deymi-Dashtebayaz, M.; Farahnak, M.; Tayyeban, E.; Moraffa, M.; Rahbari, H.R. Experimental optimization of replacing R22 with R417A without any other changes in configuration of residential air-conditioning systems based on energy and exergy analysis. *Environ. Prog. Sustain. Energy* **2023**, *42*, e14058. [CrossRef]
19. Torrella, E.; Cabello, R.; Sánchez, D.; Larumbe, J.A.; Llopis, R. On-site study of HCFC-22 substitution for HFC non-azeotropic blends (R417A, R422D) on a water chiller of a centralized HVAC system. *Energy Build.* **2010**, *42*, 1561–1566. [CrossRef]
20. Shaik, S.V.; Babu, T.P.A. Theoretical Computation of Performance of Sustainable Energy Efficient R22 Alternatives for Residential Air Conditioners. *Energy Procedia* **2017**, *138*, 710–716. [CrossRef]
21. Shaik, S.V.; Babu, T.P.A. Theoretical Performance Investigation of Vapour Compression Refrigeration System Using HFC and HC Refrigerant Mixtures as Alternatives to Replace R22. *Energy Procedia* **2017**, *109*, 235–242. [CrossRef]
22. Kalaiselvam, S.; Saravanan, R. Exergy analysis of scroll compressors working with R22, R407C and R471A as refrigerant for HVAC System. *Therm. Sci.* **2009**, *13*, 175–184. [CrossRef]
23. Wang, Z.; Wang, F.; Ma, Z.; Song, M. Numerical study on the operating performances of a novel frost-free air-source heat pump unit using three different types of refrigerant. *Appl. Therm. Eng.* **2017**, *112*, 248–258. [CrossRef]
24. Abdulqadir, I.F.; Salim, B.; Ali, O.M. Performance Investigation of Refrigerant R-407C as a Replacement to Refrigerant R22 in Window Air Conditioner Unit. *J. Civ. Eng. Front.* **2020**, *1*, 37–42. [CrossRef]
25. Fatouh, M.; Ibrahim, T.A.; Mostafa, A. Performance assessment of a direct expansion air conditioner working with R407C as an R22 alternative. *Appl. Therm. Eng.* **2010**, *30*, 127–133. [CrossRef]

26. Lee, D.Y.; Ahn, Y.; Kim, Y.; Kim, Y.; Chang, Y.S.; Nam, L. Experimental investigation on the drop-in performance of R407C as a substitute for R22 in a screw chiller with shell-and-tube heat exchangers. *Int. J. Refrig.* **2002**, *25*, 575–585. [CrossRef]
27. Aprea, C.; Greco, A. An exergetic analysis of R22 substitution. *Appl. Therm. Eng.* **2002**, *22*, 1455–1469. [CrossRef]
28. Aprea, C.; Greco, A. Performance evaluation of R22 and R407C in a vapour compression plant with reciprocating compressor. *Appl. Therm. Eng.* **2003**, *23*, 215–227. [CrossRef]
29. Cabello, R.; Torrella, E.; Navarro-Esbrí, J. Experimental evaluation of a vapour compression plant performance using R134a, R407C and R22 as working fluids. *Appl. Therm. Eng.* **2004**, *24*, 1905–1917. [CrossRef]
30. Devotta, S.; Padalkar, A.S.; Sane, N.K. Performance assessment of HCFC-22 window air conditioner retrofitted with R-407C. *Appl. Therm. Eng.* **2005**, *25*, 2937–2949. [CrossRef]
31. Zhang, C.; Liu, M.; Mohammadzadeh, A.; Taghavifar, H. A fractional adaptive type-2 fuzzy structural control system: Theoretical/experimental study. *Structures* **2024**, *70*, 107843. [CrossRef]
32. Zhang, C.; Du, C.; Sakthivel, R.; Mohammadzadeh, A. Observer-based type-3 fuzzy control for gyroscopes: Experimental/theoretical study. *Inf. Sci.* **2025**, *702*, 121907. [CrossRef]
33. Qi, H.; Zhou, Y.; Zhang, Z.; Wang, B.; Zhang, Y.; Cui, H.; Wang, X. Heat Transfer Performance in Energy Piles in Urban Areas: Case Studies for Lambeth College and Shell Centre UK. *Appl. Sci.* **2020**, *10*, 5974. [CrossRef]
34. Zhang, H.; Li, K.; Liu, T.; Liu, Y.; Hu, J.; Zuo, Q.; Jiang, L. Analysis of Radial Hydraulic Forces in Centrifugal Pump Operation via Hierarchical Clustering (HC) Algorithms. *Appl. Sci.* **2025**, *15*, 10251. [CrossRef]
35. Yuan, F.; Han, Y.; Xiao, K.; Xiang, G.; Wang, Z.; Li, L.; Cheng, W.; Chen, X. Spatial Modification Optimization Methods for Harmonic Drives Using a 3D Non-Uniform Line-Contact Elastohydrodynamic Lubrication Model. *Tribol. Int.* **2025**, *214*, 111288. [CrossRef]
36. Tong, S.; Liu, Y.; Gao, X.; Cheng, N.; Du, X.; Li, P. Analysis on the compression process of multi-stage wobble plate compressor under full pressure condition. *Appl. Therm. Eng.* **2025**, *268*, 125798. [CrossRef]
37. Xia, G.; He, X.; Jia, Y.; Zhu, Y.; Tian, Z. Design of a Cylindrical Thermal Rotary Concentrator Based on Transformation Thermodynamics. *Materials* **2025**, *18*, 4440. [CrossRef]
38. Xiong, J.; Zhang, Y.; Han, M.; Wu, J.; Tian, Z. Building energy-saving mechanism for indoor cooling temperature set-point with different envelope: A case study in Guangzhou. *J. Chin. Archit. Urban.* **2023**, *5*, 0877. [CrossRef]
39. Bai, X.; Zheng, Z.; Liu, C.; Nakayama, A. An Exact Solution Based on a Three-Energy Equation Model for Gaseous Transpiration Cooling Through a Bi-Disperse Porous Medium. *ASME J. Heat Mass Transf.* **2025**, *147*, 62702. [CrossRef]
40. Hu, X.; Quan, B.; Shi, Z.; Zhao, X.; Lu, G.; Ding, Y.; Lai, J.; Qu, J.; Peng, Y.; Lu, X. Bioinspired Hierarchical Radiative-Phase Change Hybrid Cooling Composite with Record-Breaking Cooling Power. *Adv. Mater.* **2025**, *38*, e10988. [CrossRef]
41. Ross, P.J. *Taguchi Techniques for Quality Engineering*; McGraw: New York, NY, USA, 1987.
42. Roy, R.K. *Design of Experiments Using the Taguchi Approach*; John Wiley & Sons Inc.: Hoboken, NJ, USA, 2001; ISBN 978-0-471-36101-5.560.
43. Phadke, M.S. *Quality Engineering Using Robust Design*; Prentice Hall: New Jersey, NJ, USA, 1986.
44. Taguchi, G. *Taguchi Techniques for Quality Engineering*; Quality Resources: New York, NY, USA, 1987.
45. Taguchi, G. *System of Experimental Design*; Unipub/Kraus International Publications: White Plains, NY, USA, 1987; Volume 2, 1189p.
46. Kackar, R.N. Off-Line Quality Control, Parameter Design, and the Taguchi Method. *J. Qual. Technol.* **1985**, *17*, 176–188. [CrossRef]
47. Xie, X.; Tang, S.; Zhou, J.; Zhang, D.; An, J.; Wu, X. Parametric study and optimization of H-type finned tube heat exchangers with honeycomb arrangement using Taguchi method. *Appl. Therm. Eng.* **2024**, *256*, 124116. [CrossRef]
48. Ustaoglu, A.; Kursuncu, B.; Alptekin, M.; Gok, M.S. Performance optimization and parametric evaluation of the cascade vapor compression refrigeration cycle using Taguchi and ANOVA methods. *Appl. Therm. Eng.* **2020**, *180*, 115816. [CrossRef]
49. Bademlioglu, A.H.; Canbolat, A.S.; Yamankaradeniz, N.; Kaynakli, O. Investigation of parameters affecting Organic Rankine Cycle efficiency by using Taguchi and ANOVA methods. *Appl. Therm. Eng.* **2018**, *145*, 221–228. [CrossRef]
50. Cheng, S.W.Y.; Kurnia, J.C.; Ghoreishi-Madiseh, S.A.; Sasmito, A.P. Optimization of geothermal energy extraction from abandoned oil well with a novel well bottom curvature design utilizing Taguchi method. *Energy* **2019**, *188*, 116098. [CrossRef]
51. Lin, W.; Ma, Z. Using Taguchi-Fibonacci search method to optimize phase change materials enhanced buildings with integrated solar photovoltaic thermal collectors. *Energy* **2016**, *106*, 23–37. [CrossRef]
52. Chen, G.L.; Chen, G.B.; Li, Y.H.; Wu, W.T. A study of thermal pyrolysis for castor meal using the Taguchi method. *Energy* **2014**, *71*, 62–70. [CrossRef]
53. Bilen, K.; Yapici, S.; Celik, C. A Taguchi approach for investigation of heat transfer from a surface equipped with rectangular blocks. *Energy Convers Manag.* **2001**, *42*, 951–961. [CrossRef]
54. Sahin, B. A Taguchi approach for determination of optimum design parameters for a heat exchanger having circular-cross sectional pin fins. *Heat Mass Transf.* **2007**, *45*, 493–502. [CrossRef]
55. Lu, S.M.; Li, Y.C.M.; Tang, J.C. Optimum design of natural-circulation solar-waterheater by the Taguchi method. *Energy* **2003**, *28*, 741–750. [CrossRef]

56. Yun, J.Y.; Lee, K.S. Influence of design parameters on the heat transfer and flow friction characteristics of the heat exchanger with slit fins. *Int. J. Heat Mass Transf.* **2000**, *43*, 2529–2539. [CrossRef]
57. Coşkun, S.; Motorcu, A.R.; Yamankaradeniz, N.; Pulat, E. Evaluation of control parameters' effects on system performance with Taguchi method in waste heat recovery application using mechanical heat pump. *Int. J. Refrig.* **2012**, *35*, 795–809. [CrossRef]
58. Verma, V.; Murugesan, K. Optimization of solar assisted ground source heat pump system for space heating application by Taguchi method and utility concept. *Energy Build.* **2014**, *82*, 296–309. [CrossRef]
59. Li, Y.H.; Kao, W.C. Taguchi optimization of solar thermal and heat pump combisystems under five distinct climatic conditions. *Appl. Therm. Eng.* **2018**, *133*, 283–297. [CrossRef]
60. Sazon, T.A.; Zhang, Q.; Nikpey, H. Comparison of different configurations of a solar-assisted ground-source CO_2 heat pump system for space and water heating using Taguchi-Grey Relational analysis. *Energy Convers. Manag.* **2024**, *300*, 117881. [CrossRef]
61. Esen, H.; Turgut, E. Optimization of operating parameters of a ground coupled heat pump system by Taguchi method. *Energy Build.* **2015**, *107*, 329–334. [CrossRef]
62. Sivasakthivel, T.; Murugesan, K.; Thomas, H.R. Optimization of operating parameters of ground source heat pump system for space heating and cooling by Taguchi method and utility concept. *Appl. Energy* **2014**, *116*, 76–85. [CrossRef]
63. Comakli, O.; Celik, C.; Erdogan, S. Determination of optimum working conditions in heat-pumps using nonazeotropic refrigerant mixtures. *Energy Convers. Manag.* **1999**, *40*, 193–203. [CrossRef]
64. Çomaklı, O.; Comakli, K.; Ozdemir, N.; Yilmaz, M. Analysıs of heat pumps wıth zeotropıc refrıgerant mıxtures by Taguchı method. *J. Therm. Sci. Technol.* **2010**, *30*, 113–122.
65. Xin, S.; Luo, J.; Liu, J.; Zhou, Y.; Wang, K.; Wang, J. Advanced control of multi-source heat pump systems: Synergizing Taguchi experimental design with entropy weight method for multi-criteria coordination. *Energy Build.* **2025**, *348*, 116461. [CrossRef]
66. Zamen, M.; Kahani, M.; Yazdanpanahi, J.; Abedini, R.; Ahmadi, M.H. Experimental thermal investigation of bubble column humidification-dehumidification (BC-HDH) desalination combined with submerged water-source heat pump for different salinities, Taguchi analysis. *Case Stud. Therm. Eng.* **2025**, *73*, 106499. [CrossRef]
67. Mołczan, T.; Cyklis, P. Methodology for optimising the heat pump cycle based on a real-life case study. *Energy Convers. Manag.* **2025**, *323*, 119255. [CrossRef]
68. Available online: https://www.elektronika-sa.com.pl/en/products/refrigeration/suction-line-accumulators/sla-e/SLA.E.30b.16.10.2.5 (accessed on 21 April 2025).
69. Bakırcı, K.; Çomaklı, K.; Özyurt, Ö.; Yılmaz, M. Energy and exergy analyses of solar assisted heat pump. *Eng. Mach.* **2009**, *50*, 590.
70. Kaygusuz, K.; Ayhan, T. Exergy analysis of solar assisted heat pump systems for domestic heating. *Energy* **1993**, *18*, 1077–1085. [CrossRef]
71. Mitra, A. The Taguchi method. *WIREs Comp. Stat.* **2011**, *3*, 472–480. [CrossRef]
72. Varghese, B.; Philip, N. A revıew: Taguchi experıment design for Investigation of properties of concrete. *Int. J. Civ. Eng.* **2016**, *5*, 11–16.
73. Kline, S.J.; McClinctock, F.A. Describing uncertainties in single-sample experiments. *Mech. Eng.* **1953**, *75*, 3–8.

Disclaimer/Publisher's Note: The statements, opinions and data contained in all publications are solely those of the individual author(s) and contributor(s) and not of MDPI and/or the editor(s). MDPI and/or the editor(s) disclaim responsibility for any injury to people or property resulting from any ideas, methods, instructions or products referred to in the content.